Editors' Suggestion

Nonideal measurement heat engines

Abhisek Panda,[1] Felix C. Binder,[2,3] and Sai Vinjanampathy[1,4,5,*]

[1]*Department of Physics, Indian Institute of Technology Bombay, Powai, Mumbai 400076, India*

[2]*School of Physics, Trinity College Dublin, Dublin 2, Ireland*

[3]*Trinity Quantum Alliance, Unit 16, Trinity Technology and Enterprise Centre, Pearse Street, Dublin 2, D02 YN67, Ireland*

[4]*Centre for Quantum Technologies, National University of Singapore, 3 Science Drive 2, 117543 Singapore, Singapore*

[5]*Centre of Excellence in Quantum Information, Computation, Science, and Technology, Indian Institute of Technology Bombay, Powai, Mumbai 400076, India*

(Received 23 August 2023; accepted 14 November 2023; published 15 December 2023)

We discuss the role of nonideal measurements within the context of measurement engines by contrasting examples of measurement engines which have the same work output but with varying amounts of entanglement. Accounting for the cost of resetting, correlating the engine to a pointer state, and cooling the pointer state, we show that for a given work output, thermally correlated engines can outperform corresponding entanglement engines. We also show that the optimal efficiency of the thermally correlated measurement engine is achieved with a higher-temperature pointer than the pointer temperature of the optimal entanglement engine.

DOI: 10.1103/PhysRevA.108.062214

I. INTRODUCTION

Quantum heat engines are composed of a system coupled to one or more environments such that at least one party exploits quantum energetic coherence. Quantum engines with both thermal [1,2] and nonthermal [3–5] reservoirs, energetic coherence [6–11], and entanglement [12–14] have been studied to understand how quantum engines differ from their classical analogs. In this context, it is important to consider carefully the role of quantum measurement, given its central role in quantum theory. Along with a resource-theoretic characterization of thermodynamic quantum operations [15–20], a careful accounting of the energetic constraints on quantum measurements is needed to understand their role in nonequilibrium engines. Just as in the case of thermal baths, measurements can result in an apparent change of both entropy and energy with the working fluid. Such measurements and feedback have been discussed in the context of thermal engines [21–24]. Measurement and feedback have been used in the classical and quantum context to elucidate the role of information and correlations in the second law of thermodynamics [25–31]. While engines have been shown to exploit both thermal and nonclassical correlations, measurement models have not considered the thermodynamic infeasibility of projective measurements due to the inconsistency of the third law of thermodynamics and preparation of pure state pointers [32–34]. It was shown recently that when thermodynamic feasibility is taken into account, ideal measurements which correlate the system states to the pointer states become impractical and two varieties of nonideal measurements emerge as feasible measurement models [35,36].

This hence raises the natural question as to whether nonideal measurements and the enhanced performance of quantum thermal machines whose operation includes a measurement stage are compatible. Here we consider two models of quantum engines and show that indeed nonideal measurements can still be used to construct engines which consume either thermal or nonclassical correlations as fuel. Furthermore, we show that we can always construct a thermal engine that outperforms the entanglement engine presented below in terms of efficiency for the same value of average output work. We begin the next section with a brief review of ideal and nonideal measurements. In Sec. III we describe the working of a generalized measurement engine. The findings of Sec. III are exemplified in Sec. IV, where we consider a two-qubit measurement engine and compare the performance with entangled and classically correlated initial states. We discuss our results in Sec. V.

II. NONIDEAL MEASUREMENTS AND WORK COST

It is well known that ideal projective measurements on quantum systems using finite resources are incompatible with thermodynamics [35,36]. Hence, it is necessary to take the resource cost of measurement into account and consider a description of measurements that is physical. This inclusion of thermodynamics gives rise to the notion of nonideal measurements, which was studied extensively in [35,37,38]. In this paper we review the properties of ideal measurements and recently proposed models of nonideal measurements [35].

Consider a generic quantum system ρ_S and a measuring device (pointer) ρ_P. A measurement of the system is achieved by coupling it to the pointer and allowing the joint quantum state to undergo a correlating evolution from $\rho_S \otimes \rho_P$ to a correlated state ρ_{SP} [39]. Three fundamental features define an ideal projective measurement $\mathbb{I} \otimes \Pi_i$, which infers the system state from the measured pointer state [35]. The first property desired for ideal measurements is *unbiasedness*, defined as the premeasurement probability statistics of the system being

*sai@phy.iitb.ac.in

accurately reflected by the postmeasurement pointer statistics, namely,

$$\mathrm{Tr}(\mathbb{I} \otimes \Pi_i \rho_{SP}) = \rho_{ii} \, \forall \, i, \tag{1}$$

where $\rho_{ii} = \mathrm{Tr}(|i\rangle\langle i|_S \rho_S)$ are the diagonal elements of ρ_S. Second, the measurement should be *faithful*, defined by the property that the postmeasurement system state should correspond to the outcome of the pointer, namely,

$$\sum_i \mathrm{Tr}(|i\rangle\langle i| \otimes \Pi_i \rho_{SP}) = 1. \tag{2}$$

Third, ideal measurement should be *noninvasive*, defined by the property that the measurement interaction should not change the measurement statistics for the system, i.e.,

$$\mathrm{Tr}(|i\rangle\langle i| \otimes \mathbb{I} \rho_{SP}) = \rho_{ii} \, \forall \, i. \tag{3}$$

The measurement can be faithful only if the rank of the pointer obeys $\mathrm{rank}(\rho_P) \leqslant n_P/n_S$, where n_P and n_S are the dimensions of the pointer and system, respectively (both are assumed to be finite without loss of generality) [35]. Thus an ideal measurement requires a non-full-rank pointer state, but according to the third law of thermodynamics, preparation of such a state requires infinite resources [40], which makes all practical measurements nonideal. This leads to the conclusion that a practical measurement on a thermodynamic system could be unbiased or noninvasive but not both, as both properties together would also imply faithfulness [35]. In either of these cases, after imposing the condition, we can quantify the faithfulness of the measurement by following Eq. (2). This can be done by defining the correlation function $C_{\max}(\rho_{SP}) = \sum_i \mathrm{Tr}(|i\rangle\langle i| \otimes \Pi_i \rho_{SP}) < 1$, which quantifies the probability of joint measurement of the system and pointer in the same state.

In summary, both ideal measurements and pure input states are thermodynamically incompatible since they require infinite resources [32,40–44]. Thus, quantum correlations produced as a consequence of either pure initial states or non-full-rank projective measurements do not sufficiently inform us of the role of real measurements in quantum thermal machines. We address this by considering two different types of measurement engines, an entanglement-based measurement engine (EME) using entangled states as initial states and a thermally correlated measurement engine (TCME) using initial states with classical correlations compliant with a thermal distribution, both constructed from full-rank states and operated by nonideal measurements as shown in Fig. 1. In the next section we will look at full-rank quantum engines driven by unbiased and maximally faithful measurements. Likewise, we also inspect the role of noninvasive and maximally faithful measurements in quantum engines.

III. BIPARTITE MEASUREMENT ENGINES

To investigate the effect of quantum correlations on the performance of quantum thermal machines, we consider a generic bipartite quantum measurement engine which describes both EMEs and TCMEs. The working medium consist of two n_S-level systems A and B, with the joint Hamiltonian $H = H_{\mathrm{loc}} + H_{\mathrm{int}}$. The term H_{loc} is the local Hamiltonian of

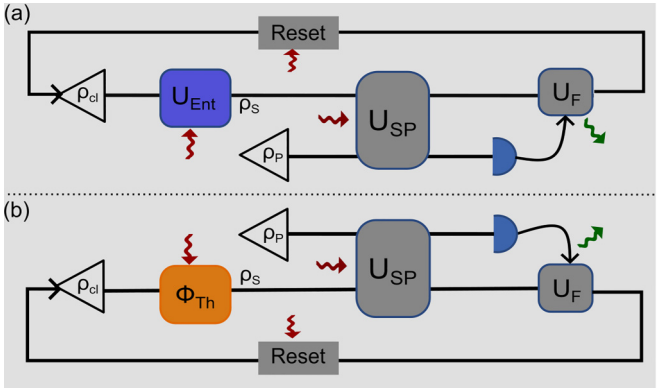

FIG. 1. The measurement engine cycle with (a) an entangled state (EME) and (b) a thermally correlated state (TCME) includes the creation of system state ρ_S, correlating it with the pointer system in state ρ_P (via U_{SP}), measurement of the pointer followed by feedback, and reset of the system to state ρ_{cl}. The energy-consuming steps are indicated by red arrows and work extraction is indicated by green arrows.

both qudits defined as

$$H_{\mathrm{loc}} = \sum_{i=0}^{n_S-1} E_i^A (|i\rangle\langle i| \otimes I) + E_i^B (I \otimes |i\rangle\langle i|), \tag{4}$$

where $\{E_i^A\}$ and $\{E_i^B\}$ are energy eigenvalues of subsystems A and B, respectively. As discussed below, appropriate feedback will extract the difference of energy eigenvalues as work; hence without loss of generality we can choose

$$E_i^B - E_j^B > E_i^A - E_j^A \geqslant 0 \, \forall \, i > j. \tag{5}$$

The interaction term H_{int} generates entanglement between the two qudits. It is generically defined as

$$H_{\mathrm{int}} = \sum_{i=0}^{n_S-1} \sum_{j=0}^{n_S-1} \frac{g_{ij}}{2} (|ij\rangle\langle ji| + |ji\rangle\langle ij|), \tag{6}$$

where g_{ij} is the coupling strength. This interaction can be switched on to prepare initial states in the EME. There is a cost associated with switching H_{int} that needs to be taken into account while running the EME. Both measurement engines operate in four stages, which we briefly review [26,45–52].

(i) State preparation. The initial states for the measurement engine are prepared from a reference product state ρ_{cl} (assumed to be diagonal). In the EME case, the entangled states are prepared by evolving the reference state with the interaction Hamiltonian, which is then turned off after creating the desired entangled state ρ_S. For the TCME, on the other hand, classical correlations are induced by a thermal completely positive and trace-preserving map. The energy cost associated with the preparation in both engines is given by $E_{\mathrm{prep}} = \mathrm{Tr}[H_{\mathrm{loc}}(\rho_S - \rho_{\mathrm{cl}})]$.

(ii) Pointer correlation. A quantum system is measured with the help of a pointer degree of freedom [53]. Since we are measuring a bipartite system, for simplicity, we consider the pointer system to be bipartite as well, governed by the

Hamiltonian

$$H_P = \sum_{i=0}^{n_P-1} E_i^{PA}(|i\rangle\langle i| \otimes I) + E_i^{PB}(I \otimes |i\rangle\langle i|). \tag{7}$$

Here E_i^{PA} and E_i^{PB} are the energy gaps of the pointer subsystems measuring systems A and B, respectively, and without loss of generality n_P is assumed to be an integer multiple of n_S. For thermodynamic consistency, we consider a full-rank pointer $\tau_P(\beta) = \tau_P = e^{-\beta H_P}/\mathrm{Tr}(e^{-\beta H_P})$, at inverse temperature β. In order to increase measurement accuracy, the pointer is initially cooled from β to $\beta' > \beta$. This process consumes the free-energy difference E_{cool} [42], which is the same for both the TCME and EME. The pointer is then correlated with the system, and the nature of the correlation matrix determines if the measurement is unbiased or noninvasive [35]. The cost associated with correlating the system to the pointer is given by

$$E_{\mathrm{corr}} = \mathrm{Tr}[(H_{\mathrm{loc}} + H_P)(\rho_{SP} - \rho_S \otimes \tau_P)]. \tag{8}$$

Here $\rho_{SP} = U_{\mathrm{corr}}(\rho_S \otimes \tau_P)U_{\mathrm{corr}}^\dagger$ and U_{corr} is the correlation matrix. The choice of U_{corr} is made such that the measurement is maximally faithful, as described below.

(iii) Work extraction. The measurement of the primary system is performed through the pointer. Based on the outcome of this pointer measurement, we then apply feedback to the system. If the pointer measurement implies that subsystem B is in a higher-energy state than subsystem A, we apply a SWAP operation and extract the work from the system. On the other hand, if the pointer reads subsystem A to be in higher-energy state than subsystem B, no feedback is applied. After extracting work, the postselected state will be given by

$$\Psi(\rho_{SP}) = \sum_{l=0}^{n_P-1}\sum_{k\geqslant l}^{n_P-1} I \otimes |kl\rangle\langle kl|\rho_{SP} I \otimes |kl\rangle\langle kl| + \sum_{l=0}^{n_P-1}\sum_{k<l}^{n_P-1} U_{\mathrm{SWAP}} \otimes |kl\rangle\langle kl|\rho_{SP}U_{\mathrm{SWAP}}^\dagger \otimes |kl\rangle\langle kl|. \tag{9}$$

Here the U_{SWAP} operator swaps the eigenstates of systems A and B, i.e., $U_{\mathrm{SWAP}}|ij\rangle = |ji\rangle\ \forall\, i, j$. The extracted work amounts to

$$W = \mathrm{Tr}\{(H_{\mathrm{loc}} + H_P)[\Psi(\rho_{SP}) - \rho_{SP}]\}. \tag{10}$$

The unavailability of non-full-rank states translates to the fact that measurements are never perfectly faithful. This results in imperfect correlations where a single pointer state can point to various system states. The imperfect correlation between the system and pointer in turn results in incorrect feedback to the system. Such incorrect feedback may correspond to either a false positive or a false negative reading of the pointer. A false positive outcome occurs when the pointer inaccurately reads that qudit B is in a higher excited state than qudit A. Thus applying a SWAP feedback results in energy consumption instead of work extraction. On the other hand, a false negative outcome occurs when qudit B is in a higher excited state than qudit A. In this scenario, a SWAP operation can extract work from the system, but the pointer detects otherwise. This leads to a lack of SWAP feedback and loss of work extraction. Thus the amount of work extracted [given by Eq. (10)] with a nonideal measurement will be less than that obtained with an ideal measurement.

(iv) Reset. After extracting work, we reset the pointer to the thermal state, but as the free energy of such a process is negative, we consider the cost of resetting the pointer to be zero. To repeat the engine cycle again we reset the system to the reference state ρ_{cl}. The minimum energy used to reset the system is given by

$$E_{\mathrm{reset}} = \mathrm{Tr}(H_{\mathrm{loc}}\{\rho_{\mathrm{cl}} - \mathrm{Tr}_P[\Psi(\rho_{SP})]\}). \tag{11}$$

As the local Hamiltonian is diagonal in the measurement basis, the work extraction and the cost associated will depend on $P_{SP}(ijkl)$, the joint system-pointer probability of the system being in $|ij\rangle$ and the pointer reading $|kl\rangle$. A noninvasive measurement can be realized if the correlation operation is of the form $U_{\mathrm{corr}} = \sum_{nm}|nm\rangle\langle nm| \otimes \tilde{U}^{nm}$. For this case, we obtain

$$P_{SP}(ijkl) = \langle ij|\rho_S|ij\rangle\langle kl|(\tilde{U}^{ij}\tau_P\tilde{U}^{\dagger ij})|kl\rangle. \tag{12}$$

Similarly, a measurement will be unbiased if $U_{\mathrm{corr}} = \sum_{nmop}|nm\rangle\langle op| \otimes |op\rangle\langle nm|\tilde{U}^{op}$, which will give

$$P_{SP}(ijkl) = \langle kl|\rho_S|kl\rangle\langle ij|(\tilde{U}^{kl}\tau_P\tilde{U}^{\dagger kl})|ij\rangle. \tag{13}$$

The faithfulness of the measurement depends on the unitary matrix $\tilde{U}^{ij}$. A maximally faithful measurement is achieved by using $\tilde{U}^{ij} = \tilde{U}^i \otimes \tilde{U}^j$, where

$$\tilde{U}^i = I - \sum_{x=0}^{\nu-1}(|x\rangle - |\nu\, i + x\rangle)(\langle x| - \langle \nu i + x|). \tag{14}$$

Here $\nu = n_P/n_S$ is assumed to be an integer without loss of generality [35]. For both types of measurement, we observe that the performance only depends on diagonal elements of the system density matrix. This indicates that while diagonal distributions preserve the work output, the impact of off-diagonal correlations on the engine performance is irrelevant. In the next section we will explore the role of correlations in the performance of quantum thermal machines by studying two-qubit measurement engines powered by either quantum or thermal correlations, respectively.

IV. TWO-QUBIT MEASUREMENT ENGINE

To compare and contrast varieties of correlations, we begin our study with an EME driven by full-rank states. To do this, we modify a recently proposed [54,55] two-qubit measurement engine to use full-rank states. A pair of qubits (labeled A and B) are taken as the working medium (system) whose evolution is governed by a Hamiltonian $H = H_{\mathrm{loc}} + H_{\mathrm{int}}$ given in Eqs. (4) and (6). To extract work from the system we consider a positive detuning $\delta = \omega_B - \omega_A$. The initial state of the system is taken as

$$\rho_{2\mathrm{qb}}(0) = (1-q)|10\rangle\langle 10| + q\frac{\mathrm{e}^{-\beta \mathrm{H}_{\mathrm{loc}}}}{Z_{\mathrm{loc}}}, \quad 0 < q \leqslant 1, \tag{15}$$

where $Z_{\mathrm{loc}} = \mathrm{Tr}[\exp(-\beta H_{\mathrm{loc}})]$. The state $\rho_{2\mathrm{qb}}(0)$ is a convex mixture of the pure state and thermal state. The admixture probability $q > 0$ in Eq. (15) guarantees that the state is full rank, circumventing the aforementioned infinite cooling cost. We let the system evolve from the initial state $\rho_{2\mathrm{qb}}(0)$ for time

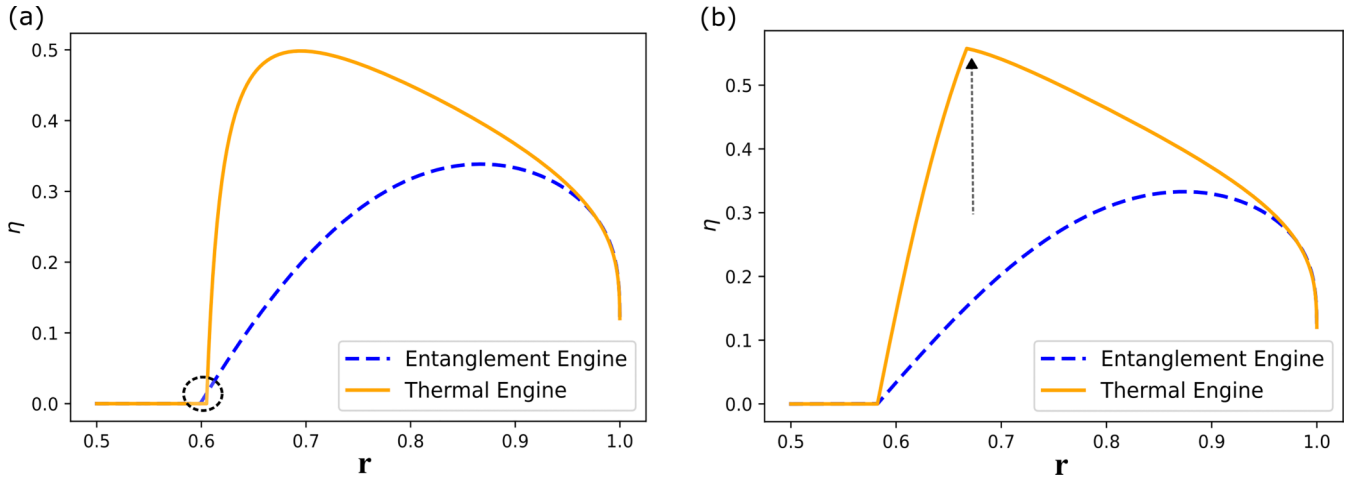

FIG. 2. Efficiency η as a function of pointer ground-state probability $\mathbf{r}$, for maximally faithful and (a) noninvasive measurement and (b) unbiased measurement. The parameters of the simulation are $\omega_A = 10$, $\delta = 50$, $\theta = \pi/4.5$, $\beta E_P = 1/30$, and $q = 0.05$. The crossover of efficiency in (a), highlighted with the dotted circle, and the kink in (b), indicated by the dotted arrow, are both discussed in the text.

$t_1 = \pi/\sqrt{g^2+\delta^2}$ such that the system state becomes as entangled as possible given the constraints on its eigenspectrum

$$\rho_{2\mathrm{qb}}(t_1) = (1-q)[\cos^2\theta|10\rangle\langle 10| + \sin^2\theta|01\rangle\langle 01| - \sin\theta\cos\theta(|10\rangle\langle 10| + |01\rangle\langle 01|)] + q\frac{e^{-\beta\tilde{H}_{\mathrm{loc}}}}{\tilde{Z}_{\mathrm{loc}}}. \tag{16}$$

Here $\tilde{H}_{\mathrm{loc}} = U_l H_{\mathrm{loc}} U_l^\dagger$, $U_l = \exp(-iH_{2\mathrm{qb}}t_1)$, $\tan\theta = g/\delta$, and $\tilde{Z}_{\mathrm{loc}} = \mathrm{Tr}[\exp(-\beta\tilde{H}_{\mathrm{loc}})]$. At this point we switch off the interaction potential, which costs energy

$$E_{\mathrm{prep}} = -\mathrm{Tr}[\rho_{2\mathrm{qb}}(t_1)H_{\mathrm{int}}]. \tag{17}$$

As we are interested in single-excitation subspace, we can use a single-qubit pointer in thermal state $\tau(\beta')$ to measure qubit B. The pointer is governed by the Hamiltonian $H_P = E_P|1\rangle\langle 1|$. To make the measurement noninvasive (or unbiased) we use $U_{\mathrm{corr}} = I \otimes U_{\mathrm{CNOT}}$ (or $U_{\mathrm{corr}} = I \otimes U_{\mathrm{unb}}$, where $U_{\mathrm{unb}} = |00\rangle\langle 00| + |01\rangle\langle 11| + |11\rangle\langle 10| + |10\rangle\langle 01|$) on the system-pointer state to correlate the pointer with qubit B. This process consumes energy given by Eq. (8). The work is extracted by applying a SWAP operation on the system qubits ($U_{\mathrm{SWAP}} = |00\rangle\langle 00| + |01\rangle\langle 10| + |10\rangle\langle 01| + |11\rangle\langle 11|$) if the pointer is observed in the excited state. The system is then reset to $\rho_{2\mathrm{qb}}(0)$ to repeat the cycle again. In order to make the measurements more accurate the pointer needs to be cooled from $\tau(\beta)$ to $\tau(\beta')$, before correlating it with the system. The free-energy difference associated with cooling can be expressed as [40,42]

$$E_{\mathrm{cool}} = \left(\frac{\beta'}{\beta} - 1\right)\left(\frac{E_P}{1+e^{-\beta' E_P}} - \frac{E_P}{1+e^{-\beta E_P}}\right). \tag{18}$$

To contrast this against thermal correlations, we now study a thermodynamically consistent TCME and demonstrate that such an engine can be designed to have better efficiency while having the same work output as the entanglement engine. Consider the initial state

$$\tilde{\rho}_{2\mathrm{qb}} = (1-q)(\cos^2\theta|10\rangle\langle 10| + \sin^2\theta|01\rangle\langle 01|) + q\frac{e^{-\beta H_{\mathrm{loc}}}}{Z_{\mathrm{loc}}}, \tag{19}$$

where $\tan^2\theta = n_{\mathrm{th}}/(n_{\mathrm{th}}+1)$ and n_{th} is average population defined below. The process of work extraction from the TCME is the same as that of the EME, but a difference arises in the reset step of both engines. The EME is reset to a reference state (15) and the TCME is reset arbitrarily close to Eq. (19) in finite time dissipatively [56],

$$\frac{d\rho}{dt} = -i[H_{\mathrm{loc}},\rho] + \gamma D[\sigma_A^+|0\rangle\langle 0|_B]\rho + \gamma D[|1\rangle\langle 1|_A\sigma_B^-]\rho + \gamma' n_{\mathrm{th}} D[|01\rangle\langle 10|]\rho + \gamma'(n_{\mathrm{th}}+1)D[|10\rangle\langle 01|]\rho. \tag{20}$$

Here $\mathcal{D}[L]X \equiv LXL^\dagger - \frac{1}{2}\{L^\dagger L, X\}$ is the usual Lindblad dissipator, $\{\gamma,\gamma'\}$ are transition rates, and $n_{\mathrm{th}} = 1/(e^{\beta(E_B-E_A)}-1)$. We choose a different initial state for the TCME as the state can be prepared and maintained using dissipators given in Eq. (20). This consumes less energy in the preparation and reset step than the EME. The energy spent in resetting (preparing) classical correlations will consume an amount of energy given by Eq. (11).

The work extracted by starting from states (16) and (19) differs by an amount proportional to the thermal admixture q. For $q \ll 1$ and $\beta > 1$, the difference in the work extracted for the TCME and EME can be made arbitrarily small to compare the efficiency of both engines directly. We plot the efficiency of the engine versus the ground-state probability of pointer $\mathbf{r}$ for two different types of measurement in Fig. 2. Efficiency is evaluated as $\eta = -W/E_{\mathrm{meas}}$, where E_{meas} is the total energy used in the measurement, i.e., $E_{\mathrm{meas}} = E_{\mathrm{prep}} + E_{\mathrm{cool}} + E_{\mathrm{corr}} + E_{\mathrm{reset}}$. We begin by noting that the graphs do not start at the origin because work output in such settings will be negative. It can be seen that the engine with the thermal initial state outperforms the engine with the entangled initial state everywhere, except for a small region near $\mathbf{r} = 0.6$ for noninvasive measurement. This is due to the fact that the

energy required in resetting the thermal state is higher than the energy required for resetting an entangled initial state for low values of purity. This region of enhanced performance by the engine with an initially entangled state decreases with decreasing admixture probability q and vanishes in the limit of $q \to 0$. As the energy costs E_{corr} and E_{cool} are similar in both engines, the observed difference in efficiency arises due to the difference in energy required to reset the states and to prepare the entangled initial state. We also note the sharp kink in the performance of the thermal engine with unbiased measurement. This is because the reset cost is negative before the kink and positive for larger $\mathbf{r}$. The negative value indicates that energy is released while resetting the system. This cost is only accounted for in the efficiency if the value is positive and considered zero if negative. If the reset cost is negative, one can choose to extract the energy as work, thereby enhancing the efficiency of the TCME. However, even without extracting this additional energy as work, the TCME has better efficiency than the EME, as shown in Fig. 2.

V. DISCUSSION

Previous approaches towards measurement engines assumed idealized measurements [54,57–59]. As such measurements are thermodynamically infeasible, one needs to model measurement with full-rank pointer states. In this paper we considered a more accurate measurement model involving states of maximal rank for both the pointer and primary system. We compared the performance of different initial states, one with entanglement and another one with thermal correlations. The realistic measurement model results in more work extraction with increasing pointer purity, but the associated cost of increasing purity eventually decreases the efficiency of the engine, which sets a trade-off between extracted work and efficiency. We found that the performance of the engine using entangled states can be matched using only classical correlations. We observed that the required purity of the pointer to operate the engine most efficiently is less in the case of thermal correlations than for entangled correlations. Hence a lower temperature bath is needed for optimal performance of the entangled engine than for the corresponding thermally correlated engine. We note that our results are consequences of the properties of measurement and hence valid for any general measurement engine where work is extracted by applying feedback (i.e., based on information obtained from measurement).

ACKNOWLEDGMENTS

F.C.B. acknowledges funding from the Irish Research Council under Grant No. IRCLA/2022/3922 and the John Templeton Foundation (Grant No. 62423). S.V. acknowledges support from a DST-SERB Early Career Research Award (Grant No. ECR/2018/000957) and DST-QUEST Grant No. DST/ICPS/QuST/Theme-4/2019. S.V. thanks A. Werulkar for useful discussions.

[1] R. Alicki, J. Phys. A: Math. Gen. **12**, L103 (1979).
[2] H. T. Quan, Y.-x. Liu, C. P. Sun, and F. Nori, Phys. Rev. E **76**, 031105 (2007).
[3] G. Manzano, F. Galve, R. Zambrini, and J. M. R. Parrondo, Phys. Rev. E **93**, 052120 (2016).
[4] W. Niedenzu, V. Mukherjee, A. Ghosh, A. G. Kofman, and G. Kurizki, Nat. Commun. **9**, 165 (2018).
[5] B. K. Agarwalla, J.-H. Jiang, and D. Segal, Phys. Rev. B **96**, 104304 (2017).
[6] K. Hammam, Y. Hassouni, R. Fazio, and G. Manzano, New J. Phys. **23**, 043024 (2021).
[7] J. Klatzow, J. N. Becker, P. M. Ledingham, C. Weinzetl, K. T. Kaczmarek, D. J. Saunders, J. Nunn, I. A. Walmsley, R. Uzdin, and E. Poem, Phys. Rev. Lett. **122**, 110601 (2019).
[8] R. Uzdin, Phys. Rev. Appl. **6**, 024004 (2016).
[9] M. O. Scully, Phys. Rev. Lett. **104**, 207701 (2010).
[10] F. Binder, S. Vinjanampathy, K. Modi, and J. Goold, Phys. Rev. E **91**, 032119 (2015).
[11] P. Kammerlander and J. Anders, Sci. Rep. **6**, 22174 (2016).
[12] X. Huang, H. Xu, X. Niu, and Y. Fu, Phys. Scr. **88**, 065008 (2013).
[13] A. Tavakoli, G. Haack, N. Brunner, and J. B. Brask, Phys. Rev. A **101**, 012315 (2020).
[14] M. Josefsson and M. Leijnse, Phys. Rev. B **101**, 081408(R) (2020).
[15] D. Janzing, P. Wocjan, R. Zeier, R. Geiss, and T. Beth, Int. J. Theor. Phys. **39**, 2717 (2000).
[16] F. G. S. L. Brandão, M. Horodecki, J. Oppenheim, J. M. Renes, and R. W. Spekkens, Phys. Rev. Lett. **111**, 250404 (2013).
[17] P. Faist, J. Oppenheim, and R. Renner, New J. Phys. **17**, 043003 (2015).
[18] F. Brandão, M. Horodecki, N. Ng, J. Oppenheim, and S. Wehner, Proc. Natl. Acad. Sci. USA **112**, 3275 (2015).
[19] M. Lostaglio, The resource theory of quantum thermodynamics, Ph.D. thesis, Imperial College London, 2016.
[20] M. P. Müller, Phys. Rev. X **8**, 041051 (2018).
[21] S. Seah, S. Nimmrichter, and V. Scarani, Phys. Rev. Lett. **124**, 100603 (2020).
[22] M. S. Alam and B. P. Venkatesh, arXiv:2201.06303.
[23] L. M. Cangemi, C. Bhadra, and A. Levy, arXiv:2302.00726.
[24] S. W. Kim, T. Sagawa, S. De Liberato, and M. Ueda, Phys. Rev. Lett. **106**, 070401 (2011).
[25] T. D. Kieu, Eur. Phys. J. D **39**, 115 (2006).
[26] C. Elouard, D. Herrera-Martí, B. Huard, and A. Auffèves, Phys. Rev. Lett. **118**, 260603 (2017).
[27] S. Vinjanampathy and K. Modi, Int. J. Quantum. Inf. **14**, 1640033 (2016).
[28] G. Francica, J. Goold, F. Plastina, and M. Paternostro, npj Quantum Inf. **3**, 12 (2017).
[29] J. P. Santos, L. C. Céleri, G. T. Landi, and M. Paternostro, npj Quantum Inf. **5**, 23 (2019).
[30] K. Jacobs, Phys. Rev. E **86**, 040106(R) (2012).
[31] S. Gherardini, F. Campaioli, F. Caruso, and F. C. Binder, Phys. Rev. Res. **2**, 013095 (2020).
[32] H. Wilming and R. Gallego, Phys. Rev. X **7**, 041033 (2017).

[33] J. Scharlau and M. P. Mueller, Quantum **2**, 54 (2018).
[34] T. D. Kieu, Phys. Lett. A **383**, 125848 (2019).
[35] Y. Guryanova, N. Friis, and M. Huber, Quantum **4**, 222 (2020).
[36] T. Debarba, G. Manzano, Y. Guryanova, M. Huber, and N. Friis, New J. Phys. **21**, 113002 (2019).
[37] M. H. Mohammady and T. Miyadera, Phys. Rev. A **107**, 022406 (2023).
[38] P. Busch, P. J. Lahti, and P. Mittelstaedt, *The Quantum Theory of Measurement*, Lecture Notes in Physics Monographs Vol. 2 (Springer, Berlin, 1996), Chap. III, pp. 25–90.
[39] G. Sewell, in *Quantum Theory*, edited by G. Adenier, A. Y. Khrennikov, P. Lahti, V. I. Man'ko, and T. M. Nieuwenhuizen, AIP Conference Proceedings No. 962 (American Institute of Physics, Melville, 2007), pp. 215–222.
[40] P. Taranto, F. Bakhshinezhad, A. Bluhm, R. Silva, N. Friis, M. P. E. Lock, G. Vitagliano, F. C. Binder, T. Debarba, E. Schwarzhans, F. Clivaz, and M. Huber, PRX Quantum **4**, 010332 (2023).
[41] L. Masanes and J. Oppenheim, Nat. Commun. **8**, 14538 (2017).
[42] F. Clivaz, R. Silva, G. Haack, J. B. Brask, N. Brunner, and M. Huber, Phys. Rev. Lett. **123**, 170605 (2019).
[43] A. E. Allahverdyan, K. V. Hovhannisyan, D. Janzing, and G. Mahler, Phys. Rev. E **84**, 041109 (2011).
[44] S. Vinjanampathy and J. Anders, Contemp. Phys. **57**, 545 (2016).
[45] M. H. Mohammady and J. Anders, New J. Phys. **19**, 113026 (2017).
[46] K. Ito, P. Talkner, B. P. Venkatesh, and G. Watanabe, Phys. Rev. A **99**, 032117 (2019).
[47] A. N. Jordan, C. Elouard, and A. Auffèves, Quantum Stud.: Math. Found. **7**, 203 (2020).
[48] X. Ding, J. Yi, Y. W. Kim, and P. Talkner, Phys. Rev. E **98**, 042122 (2018).
[49] J. Yi, P. Talkner, and Y. W. Kim, Phys. Rev. E **96**, 022108 (2017).
[50] C. Elouard and A. N. Jordan, Phys. Rev. Lett. **120**, 260601 (2018).
[51] J. Son, P. Talkner, and J. Thingna, PRX Quantum **2**, 040328 (2021).
[52] J. Thingna and P. Talkner, Phys. Rev. A **102**, 012213 (2020).
[53] J. von Neumann, in *Mathematical Foundations of Quantum Mechanics*, edited by N. A. Wheeler (Princeton University Press, Princeton, 2018), Vol. 53, pp. 437–445.
[54] L. Bresque, P. A. Camati, S. Rogers, K. Murch, A. N. Jordan, and A. Auffèves, Phys. Rev. Lett. **126**, 120605 (2021).
[55] X. L. Huang, A. N. Yang, H. W. Zhang, S. Q. Zhao, and S. L. Wu, Quantum Inf. Process. **19**, 242 (2020).
[56] H.-P. Breuer and F. Petruccione, *The Theory of Open Quantum Systems* (Oxford University Press, Oxford, 2002).
[57] Z. Lin, S. Su, J. Chen, J. Chen, and J. F. G. Santos, Phys. Rev. A **104**, 062210 (2021).
[58] J. Roßnagel, O. Abah, F. Schmidt-Kaler, K. Singer, and E. Lutz, Phys. Rev. Lett. **112**, 030602 (2014).
[59] I. Khait, J. Carrasquilla, and D. Segal, Phys. Rev. Res. **4**, L012029 (2022).